PREDICTIONS FOR RADIATION SHIELDING MATERIALS

SUMMARY OF RESEARCH

NASA Cooperative Agreement NCC-1-327

December 19, 1998 to December 18, 2002

Principal Investigator: Richard L. Kiefer

Address:
Department of Chemistry
College of William and Mary
P.O. Box 8795
Williamsburg, VA 23187-8795

Predictions for Radiation-Shielding Materials

Introduction

Radiation from galactic cosmic rays (GCR) and solar particle events (SPE) is a serious hazard to humans and electronic instruments during space travel, particularly on prolonged missions outside the Earth's magnetic fields. Galactic cosmic radiation (GCR) is composed of ~98% nucleons and ~2% electrons and positrons (ref. 1). Although cosmic ray heavy ions are 1~2% of the fluence, these energetic heavy nuclei (HZE) contribute 50% of the long-term dose (ref. 2). These unusually high specific ionizations pose a significant health hazard acting as carcinogens and also causing microelectronics damage inside spacecraft and high-flying aircraft. These HZE ions are of concern for radiation protection and radiation shielding technology, because gross rearrangements and mutations and deletions in DNA are expected. Calculations have shown that HZE particles have a strong preference for interaction with light nuclei (ref. 3). The best shield for this radiation would be liquid hydrogen, which is totally impractical. For this reason, hydrogen-containing polymers make the most effective practical shields.

Shielding is required during missions in Earth orbit and possibly for frequent flying at high altitude because of the broad GCR spectrum and during a passage into deep space and Lunar/Mars habitation because of the protracted exposure encountered on a long space mission. An additional hazzard comes from solar particle events (SPEs) which are mostly energetic protons that can produce heavy ion secondaries as well as neutrons in materials. These events occur at unpredictable times and can deliver a potentially lethal dose within several hours to an unshielded human.

Radiation protection for humans requires safety in short-term missions and maintaining career exposure limits within acceptable levels on future long-term exploration missions. The selection of shield materials can alter the protection of humans by an order of magnitude (ref. 4). If improperly selected, shielding materials can actually increase radiation damage due to penetration properties and nuclear fragmentation (ref. 4). Protecting space-borne microelectronics from single event upsets (SEUs) by transmitted radiation will benefit system reliability and system design cost by using optimal shield materials.

Long-term missions on the surface of the Moon or Mars will require the construction of habitats to protect humans during their stay. One approach to the construction is to make structural materials from lunar or Martian regolith using a polymeric material as a binder. The hydrogen-containing polymers are considerably more effective for radiation protection than the regolith (ref. 5), but the combination minimizes the amount of polymer to be transported. We have made composites of simulated lunar regolith with two different polymers, LaRC-SI, a high-performance polyimide thermoset, and polyethylene, a thermoplastic.

Polymer/Regolith Structural Materials

Simulated lunar regolith resembles surface materials from the Apollo 11 site on the Moon and is made by crushing, grinding, and sieving 1.1 billion-year old basaltic rock from Minnesota. It is prepared and sold by the Department of Geology and Geophysics at the University of Minnesota, Twin Cities. The first specimens we made were composites of the simulant and LaRC-SI, a high-performance polyimide developed at the NASA Langley Research Center (ref. 6).

Polyimides are a class of polymers used in a variety of high performance/high temperature applications which include adhesives, matrix resins for composites, and high strength films and coatings (ref. 7). Various polyimides have been developed with distinct processing advantages, and mechanical and physical properties. Many polyimide thermoplastics are insoluble in common organic solvents and are solution processed in the polyamic acid state, which has the disadvantages of unstableness, susceptibility to hydrolysis, and water production during imidization. Langley Research Center developed the soluble amorphous aromatic thermoplastic polyimide, LaRC™-SI. This polyimide is soluble in N-methylpyrrolidinone (NMP) at elevated temperatures and soluble up to at least 40% solids at room temperature (ref. 6), which gives the processing advantage of making composites in solvents generally used in solution processing. Because of its excellent adhesive and dielectric properties, there are numerous applications of this material. IMITEC, INC is licensed to manufacture LaRC™-SI. This polymer was also chosen because there was much local expertise at LaRC for its processing in a heated press.

Specimens of LaRC-SI and regolith were made by thoroughly mixing the regolith and polymer powders and placing the mixture in a steel mold which had been coated with a release agent. In addition to the release agent, pieces of Kapton film were placed on the bottom of the mold and on top of the powder before the plunger was inserted. The Kapton film was also coated with the release agent. The mold was then placed in a heated press with just enough pressure to keep the top and bottom platens in contact with the mold. The temperature was raised to 325° C, which is about 10 degrees above the melting point of the polymer. The pressure was then slowly increased to 385 psi and the temperature was held for 60 to 90 minutes depending on the thickness and composition of the specimen. The shorter time was used for thin specimens and those with 50% on more LaRC-SI, while the longer time was used for thick specimens and those with low (< 50%) polymer content. After the appropriate curing time, the specimen was cooled under pressure until the temperature was 120° C. Specimens with polymer/regolith compositions of 90/10, 80/20, 70/30, 60/40, 50/50, 40/60, 30/70, 20/80, and 15/85 were made using this procedure. When the polymer composition went below 15%, the specimen had no structural integrity and crumbled easily. With this process, samples up to 15.2 x 15.2 x 0.64 cm (6 x 6 x 0.25 in)were made and tested. By making these samples, we were able to show that good structural materials could be made from regolith with a polymer binder.

The average temperature on the surface of Mars is about - 40° C, so a polymer with a high melting point is not necessary. Further, a high processing temperature is detrimental to making the materials on the Martian surface. Thus, we expanded our study to develop a process for making composites with polyethylene and regolith. A medium density polyethylene powder was purchased from Aldrich Chemical Company. The polymer had a melting range of 109 to 111°C. With polyethylene as the polymer, the material was heated from 115° to118° C at a pressure of 100 psi, held for up to one hour, and cooled to about 50° C before the pressure was released. Specimens with polymer/regolith compositions of 25/75, 20,80, 15/85, 10/90, 7/93, and 5/95 were made. For polyethylene compositions above 25%, leakage of the polymer from the mold became so severe that an accurate composite composition was not possible. Specimens of various size up to 15.2 x 15.2 x 0.64 cm were made and tested. Polyethylene, with its empirical formula CH_2, contains the highest amount of hydrogen of any polymer. This in addition to its lower processing temperature, makes polyethylene an ideal polymer for making regolith composites for Martian or lunar habitats.

Computational Methods for Shield Selection

Ions of GCR are not reduced in number but are modified by the presence of shield materials (ref. 3). The modifications depend on the shielding nuclear properties of the different shield materials. The NASA Langley Research Center (LaRC) has developed transport codes and an interaction database for HZE and nucleonic components (ref. 2). This code system and database provides a state-of-the-art environment/shield materials analysis tool for engineering design and mission planning by predicting the local radiation environments and linear energy transfer (LET) spectra at critical sites behind candidate shield materials. Radiation effects behind various materials were assessed using NASA-developed bioresponse models to examine the effectiveness of these materials.

Changes in environmental components were understood qualitatively as a function of shield composition (ref. 4). The role of nuclear cross sections in modifying the radiation fields and the associated effects on the microscopic distribution of the energy absorption events were investigated to study the attenuation characteristics of the GCR in a tissue equivalent shield (ref. 4). The changes by shielding materials on microscopic fluctuations will serve as a primary means of radiation protection. Theoretically, a liquid hydrogen shield is an optimal selection for lowering the LET pivot point to enhance the shield performance (ref. 4). Therefore, hydrogen-containing materials, such as polymers, should be very effective in reducing radiation risk.

The effects on two biological response models were examined to compare shield effectiveness of some materials with one-element in protection from GCR exposure (ref. 4). The rates of attenuation of biological effects between the conventional dosimetry and track structure repair models agree well only for the liquid hydrogen shield (ref. 4). Discrepancy between the two risk models is increased with the shield atomic number for non-hydrogenous shields. An effective shielding element is identified from this result (ref. 4), even though it increases the low LET radiation fields for which the effects are due primarily to indirect damage in cellular DNA brought about by OH radicals. The significance of the effect is negligible (ref. 8). Therefore, the use of high-performance polymer composites is attractive for vehicle construction because of excellent mechanical properties as well as radiation shielding capability.

The estimation of risk to humans depends on the reliability of the nuclear fragmentation database and the accurate representation of the geometry for the critical regions. Human geometry of CAM (Computerized Anatomical Man Model, ref. 9) has been added into the HZETRN code to improve the evaluation method at critical body tissues behind shield materials. The fast computational transport codes and their nuclear models are constantly being improved and validated. Effects of shielding materials on bioresponse at critical regions was examined by using improved models for the development of shield materials concepts.

SEU cross sections are measured by experiment. The most effective shields for SEU reduction are also materials with high hydrogen density, such as polyethylene (ref. 10). Candidate materials, as a load-bearing structural piece or as a container or coating for microelectronics, were compared to determine the maximum reduction in the SEU rate.

For the purpose of identifying shield materials on the Martian surface, Martian meteorites and Martian regolith were considered to be representative of Martian rocks and soil respectively. Using the HZETRN code, predictions of the annual dose equivalent behind various types of Martian meteorites and Martian regolith were made (ref. 5). The results show that there is essentially no difference between the meteorites and the regolith in shielding properties, so regolith can be considered to be an accurate representation of typical Martian surface materials and is used as the *in situ* Martian habitat/shielding material in all further analyses.

A second model, a track structure repair kinetic model (ref. 11), was used to compare shield materials. This model uses several biological systems for which a large body of experimental data exists with various ions and in which repair kinetic studies were made. For our studies, cell death and neoplastic transformation in C3H10T1/2 mouse cells, and Harderian gland tumor induction in mice were used to compare the shielding properties of Martian regolith and aluminum. The results shown in Table 1 show the performance of the two materials to be virtually the same with a modest reduction in cell death rate at thicknesses of 10 mg/cm^2 and greater relative to free space. The transformation rate and tumor prevalence increase relative to free space, but the value decreases with increasing thickness. This is a result of an increased number of particles due to fragmentation in the shield. Thus, there would be no reason to transport aluminum to Mars since the regolith is an equally effective shield and can be made into structural materials *in situ*.

The effectiveness of regolith as a shield can be enhanced with a polymer binder since polymers have a significant amount of hydrogen. The shielding effects of adding varying amounts of polymer to regolith was examined using composites containing 10, 20, 30, and 40% polymer by weight. The results are shown in Figure 1 where it is clear that the addition of polymer enhances the shielding properties of the regolith. The polymer chosen was LaRC-SI since it was the first polymer used to make composite materials with regolith.

All calculations were performed by Dr. Myung-Hee Y. Kim, a postdoctoral research associate who was supported by this cooperative agreement.

Laboratory Tests on the Materials

Heavy-ion beams can be used to acquire the required knowledge in a ground-based laboratory and to analyze the radiation of a baseline exploration mission. In a NASA space radiation research program in collaboration with the Brookhaven National Laboratory (BNL), ^{56}Fe beams are used at the Alternating Gradient Synchrotron (AGS) at BNL. The beam energy of the BNL ^{56}Fe experiment is 1.05 A GeV. It is near the peak of the solar-modulated GCR ^{56}Fe energy spectrum for simulation of space radiation. LaRC™-SI and in-situ simulant will be used to make composites as shield and construction materials for Moon/Mars-based habitation. Some preliminary dose reduction data on a series of targets, including Martian regolith, exposed to a ^{56}Fe beam at BNL are shown in Figure 2. These data were obtained by Dr. Carey Zeitlin and Dr. Jack Miller of the Lawrence Berkeley Laboratory who were funded by a NASA grant. Surprisingly, the best target for dose reduction was an epoxy, with polymer/regolith composite third. However, these are simple experiments looking at dose behind some depth of material and do not have any corrections for biological damage.

Two composite targets were irradiated with nearly monoenergetic 55 MeV proton beams produced at the Texas A&M University Cyclotron facility. The number of single event upsets (SEU) in a 4 MB MCM6246-5V Static Random Access Memory (SRAM) chip was measured for the specimens with the 55 MeV proton beam at several fluence levels between 1×10^7 p/cm^2 to 4×10^9 p/cm^2 as shown in Figure 3. As the fluences are increased to 5×10^7 p/cm^2, measurable errors are observed. The results show clearly that specimen 101 with 40% LaRC-SI by mass is much better than specimen 102 with 20% LaRC-SI for shielding as the fluence of the beam reaches 4×10^9 /cm^2. It is reasoned that each linear energy transfer (LET) component of a given particle behind the 40% LaRC-SI specimen, which represents radiation quality, is attenuated faster than that behind the 20% LaRC-SI specimen. Therefore, the 40% LaRC-SI specimen is more effective in shielding the SRAM from 55 MeV proton beams. The thick composites with 40 wt% LaRC-SI are also expected to be more effective than those with 20 wt% LaRC-SI to shield other heavier particles.

SEU measurements behind the two specimens and a polyethylene target were also taken at the Los Alamos Nuclear Science Center (LANSCE) in a neutron beam with energy up to 800 MeV. The results compared to measurements without any shield are shown in Table 2. Because of the secondary particle production by regolith/LaRC-SI composites, more SEU are produced behind the two specimens than with no shield. When the beam was focused on the first set of chips (1, 2, and 4), polyethylene showed improved shielding effectiveness possibly because of the decreased original beam intensity as predicted in the theoretical calculation (ref. 5). But, a large number of secondary particles generates more SEUs than with no shield as shown in the second set of chips (20, 40, and 80). These results are within statistical error and more experimental data are required to get a qualitative conclusion.

For the characterization of composites, thermomechanical analysis (TMA) and thermogravimetric analysis (TGA) were used to measure the glass transition temperature (T_g) and mass loss, respectively. The glass transition temperatures measured by TMA are shown in Figure 4 and they indicate that these composites should contain good mechanical properties up to at least 223 °C. The temperatures at 5% mass loss and 10% mass loss measured by TGA in this figure show that mass loss temperatures are increased as the amount of LaRC-SI decreases due to the smaller erosion rate of the polymer in the composites. These data indicate that the composites are reasonably stable at high temperature.

Structural properties of maximum load, Young's modulus, and ultimate compression strength were measured for the specimens before and after beam tests and these are shown in Figure 5 for 40%/60% LaRC-SI/regolith (sample101) specimens on the left-hand side and for 20%/80% LaRC-SI/regolith (sample102) specimens on the right-hand side. It can be seen in Figure 5(b), that there was some degradation in the Young's modulus for the neutron-exposed specimens. The Young's modulus of neutron-exposed specimens for both regolith 101 and 102 were decreased by 10% from the baseline. Those for regolith 102 had a wider distribution than those for regolith 101 due to the non-uniformity of each specimen. By contrast, the proton-exposed specimens for both regolith 101 and 102 composites experienced an increase in the Young's modulus possibly due to the crosslinking between polymer molecules. These composites have a reasonable range of structural properties in addition to the increased radiation protection from a 55 MeV proton beam. The irradiations and compression tests were done by Jerod Moore of Praire View A&M University under a NASA grant.

Specimens of polyethylene/regolith in various combinations were characterized by thermomechanical analysis to determine their softening temperatures. Samples with polyethylene contents of 5%, 7%, 10%, 15%, and 20% were analyzed. Not surprisingly, all samples softened at about the same temperature, 112° C, slightly higher than the melting point of the polymer.

Compression tests were performed on specimens of the same composition as above in addition to pure polyethylene. The ultimate compressive strength was calculated for each specimen by dividing the maximum load that the sample withstood by its cross-sectional area. Similarly, the compressive yield strength was determined by dividing the load point yield by the cross-sectional area. The compressive chord modulus of elasticity for each sample was measured as the slope of the linear part of the stress-strain curve. The results of these determinations are shown in Figures 6, 7, and 8, for the ultimate compressive strength, compressive yield strength, and the compressive chord modulus of elasticity respectively. Two different compression rates were used, 0.127 cm/min and 0.0203 cm/min. The slower rate was introduced when it became obvious that the specimens with low polyethylene content failed in such a short time with the original rate that good results could not be obtained. It is clear from Figures 6 to 8 that the strongest specimens in terms of compression were those with 10%/90% polyethylene/regolith. Too little polyethylene would result in a composite that crumbles easily, and apparently too much polyethylene results in a composite with reduced stiffness.

Conclusions

Shield transport properties show that polymers are superior to metals (including standard aluminum construction materials) in removing the high LET components without adding greatly to the low LET radiation fields (ref. 12). Regolith attenuates the high LET components but adds to the low LET fields. Calculations show that Martian regolith is equal in shielding effectiveness to Martian rocks, so regolith can be used in calculations and in experiments as a good representation of material on the Martian surface. Calculations of biological response behind shields of Martian regolith and aluminum of varying thicknesses show that the two materials give virtually the same results for C3H10T1/2 cell death rate and transformation rate, and for excess Harderian gland tumor prevalence. Calculations have also shown that the biological response behind polymer/regolith composites decreases with increasing polymer content indicating that hydrogen-containing polymers could play an important role in GCR shielding on Mars.

Composites of LaRC-SI/regolith and polyethylene/regolith are shown to have good structural properties as well as being effective shields from GCR radiation. Thus, it would not be necessary to transport aluminum to Mars to build habitats, since the regolith alone is as effective a shield as aluminum and this is enhanced by the addition of polymer to make structural materials.

References

1. J. A. Simpson, Introduction to the Galactic Cosmic Radiation. Composition and Origin of Cosmic Rays, Maurice M. Shapiro, ed., D. Reidel Publ. Co. 1-24 (1983)

2. J. W. Wilson, L. W. Townsend, W. Schimmerling, G. S. Khandelwal, F. Khan, J. E. Nealy, F. A. Cucinotta, L. C. Simonsen, J. L. Shinn and J. W. Norbury, Transport Methods and Interactions for Space Radiations, NASA RP-1257 (1991)

3. M. Y. Kim, J. W. Wilson, S. A. Thibeault, J. E. Nealy, F. F. Badavi and R. L. Kiefer, Performance Study of Galactic Cosmic Ray Shield Materials, NASA TP-3473 (1994)

4. J. W. Wilson, M. Y. Kim, W. Schimmerling, F. F. Badavi, S. A. Thibeault, F. A. Cucinotta, J. L. Shinn and R. L. Kiefer, Issues in Space Radiation Protection: Galactic Cosmic Rays, Health Phys. **68**(1), 50-58 (1995)

5. M.-H. Y. Kim, S. A. Thibeault, J. W. Wilson, L. C. Simonsen, L. Heilbronn, K. Chang, R. L. Kiefer, J. A. Weakley, and H. G. Maahs, Development and Testing of *in situ* Materials for Human Exploration of Mars, High Perform. Polym. **12**, *13-26, (2000)*

6. Bryant, R. G.: A Soluble Copolyimide, Polym. Prep., vol. 35, n. 1, 1994, pp. 517-518.

7. Blackie, Glasgow, and London: “Polyimides”, Wilson, D.; Stenzenberger, D.; and Hergenrother, P. M. Eds., 1990.

8. D. Billen, Commentary: Spontaneous DNA Damage and Its Significance for the "Negligible Dose" Controversy in Radiation Protection, Radiation Research **124**, 242-245 (1990)

9. Atwell, W.; Weyland, M. D.; and Simonsen, L. C.: Solar Particle Dose Rate Buildup and Distribution in Critical Body Organs. *Biological Effects and Physics of Solar and Galactic Cosmic Radiation*. Part B., C. E. Swenberg, G. Horneck, and E. G. Stassinopoulos, eds., Plenum Press, pp. 831-844, 1993

10. M. Y. Kim, J. L. Shinn, J. W. Wilson, S. A. Thibeault, R. A. Orwoll and R. L. Kiefer, Effects of Shield Materials on Calculated Single Event Upset Rate for Static Random Access Memory Exposed to Energetic Ions, Bull. Am. Phys. Soc., **39**(8), 1821 (1994)

11. International Commission for Radiological Protection 1991, *1990 Recommendation of the InternationalCommission on Radiobiological Protection (ICRP Publication 60)* (Oxford: Pergamon)

12. W. Schimmerling, J. W. Wilson, M. Y. Kim, J. E. Nealy, S. A. Thibeault, F. A. Cucinotta, J. L. Shinn and R. L. Kiefer, Shielding Against Galactic Cosmic Rays, Adv. Space Res. **17**, **No. 2**, 31-36 (1996)

Table 1. The biological responses behind Martian regolith and aluminum shields after a one year GCR exposure.

Thickness ($g\ cm^{-2}$)	C3H10T1/2 cell death rate	C3H10T1/2 cell transformation rate	Excess Harderian gland tumor prevalence (%)
Martian regolith			
Free space	3.18×10^{-2}	1.13×10^{-5}	2.23
1	3.92×10^{-2}	1.74×10^{-5}	3.50
5	3.28×10^{-2}	1.65×10^{-5}	3.28
10	2.74×10^{-2}	1.54×10^{-5}	3.02
30	1.89×10^{-2}	1.34×10^{-5}	2.63
50	1.65×10^{-2}	1.29×10^{-5}	2.56
Aluminum			
Free space	3.18×10^{-2}	1.13×10^{-5}	2.23
1	3.94×10^{-2}	1.76×10^{-5}	3.57
5	3.33×10^{-2}	1.70×10^{-5}	3.37
10	2.80×10^{-2}	1.59×10^{-5}	3.12
30	1.91×10^{-2}	1.39×10^{-5}	2.73
50	1.65×10^{-2}	1.33×10^{-5}	2.63

Table 2. Single Event Upset (SEU) measurement behind shield materials irradiated with LANSCE neutron beams

Shield Material	Beam Focused on Chips 1, 2, 4	Beam Focused on Chips 20, 40, 80
No Shield	474	401
Specimen 101	580	483
Specimen 102	633	428
Polyethylene	454	446

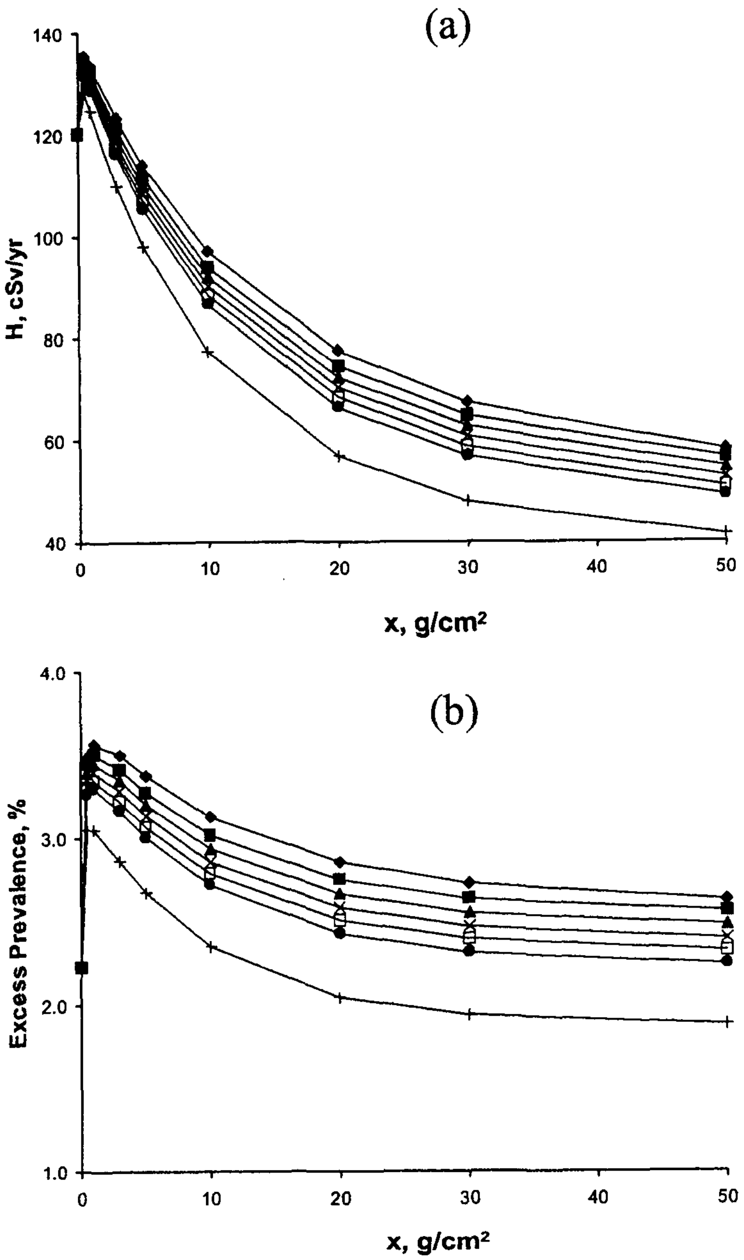

Figure 1. Biological response behind various materials after 1-year GCR exposure (a) dose equivalent and (b) excess Harderian Gland tumor prevalence.
(◆: Aluminum; ■: Martian regolith; ▲: Martian regolith/LaRC™-SI composite of 90%/10% by weight; ×: 80%/20% composite; □: 70%/30% composite; ●: 60%/40% composite; +: LaRC™-SI)

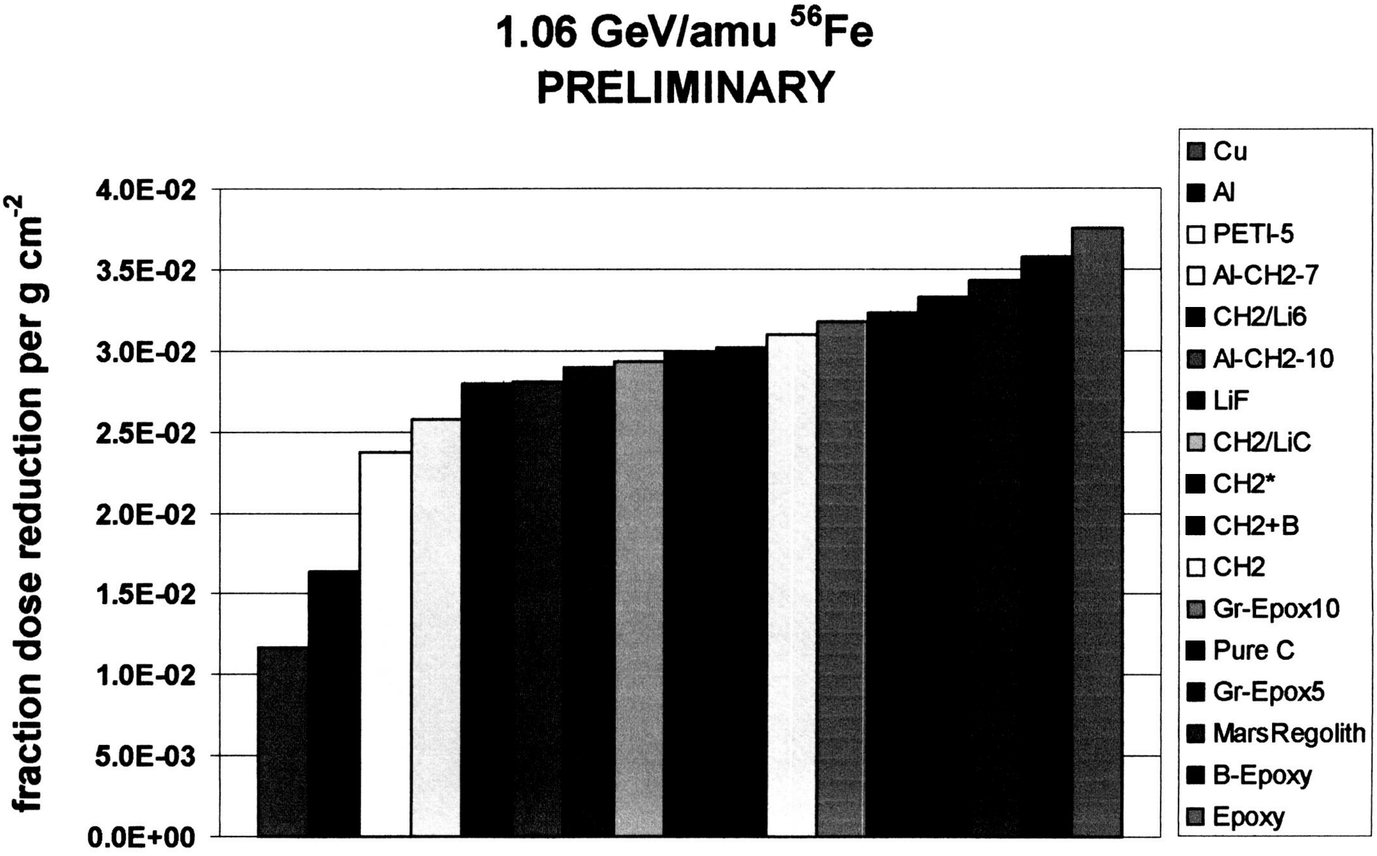

Figure 2. Preliminary dose reduction results from 1.06 GeV/amu ^{56}Fe ions on various targets. CH_2 is polyethylene.

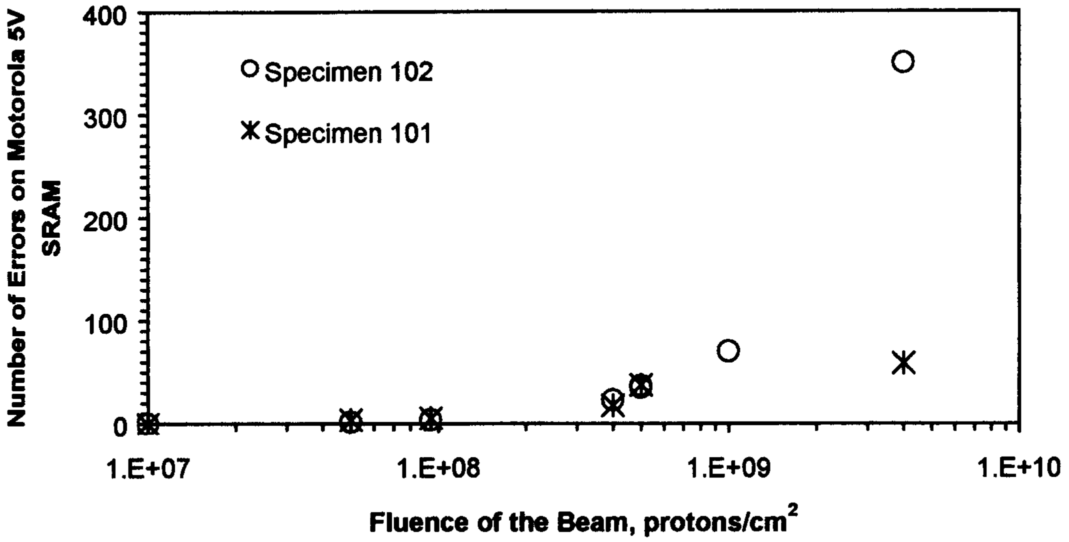

Figure 3. Single event upsets on Motorola MCM6246-5V SRAM from 55-MeV proton beams behind regolith/LaRC-SI microcomposite shields.

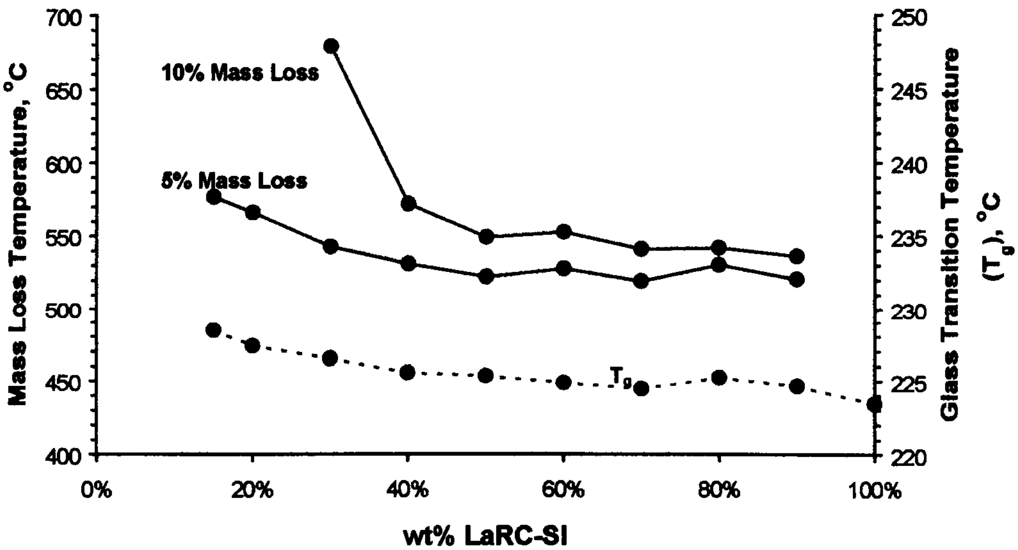

Figure 4. TGA mass loss and TMA glass transition temperature for regolith/LaRC-SI microcomposite shields.

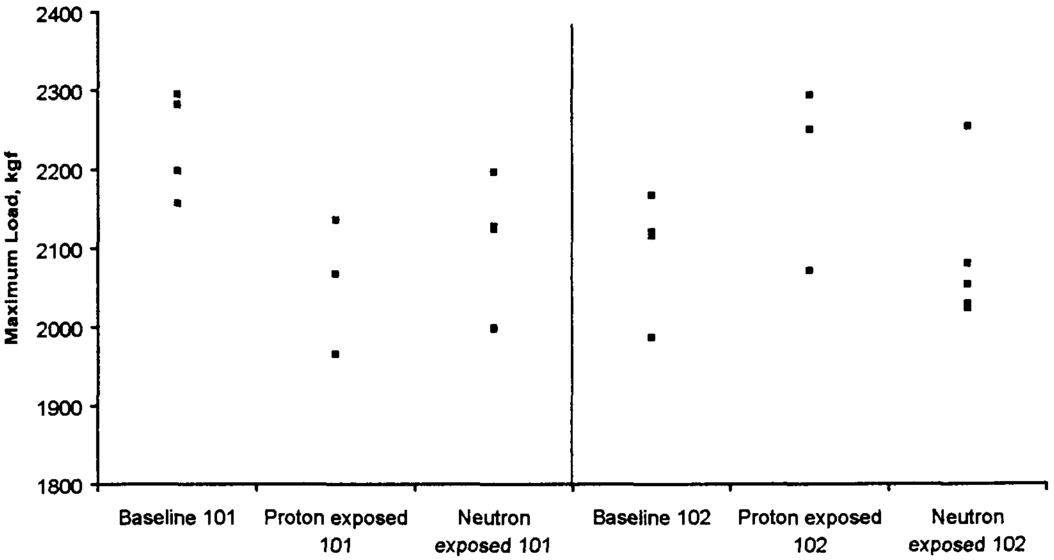

Figure 5(a). Maximum load for regolith 101 specimens on left-hand side and for regolith 102 specimens on right-hand side.

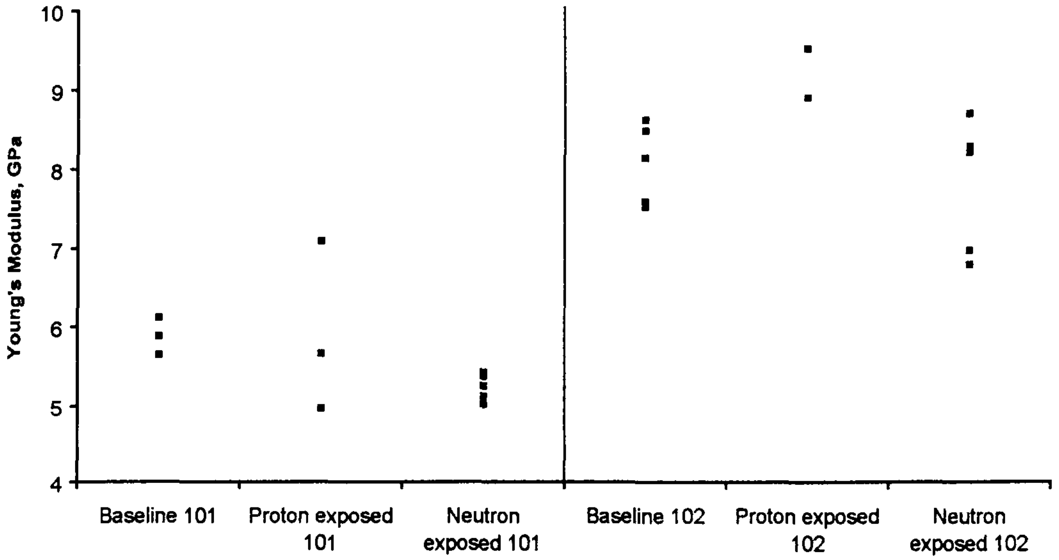

Figure 5(b). Young's modulus for regolith 101 specimens on left-hand side and for regolith 102 specimens on right-hand side.

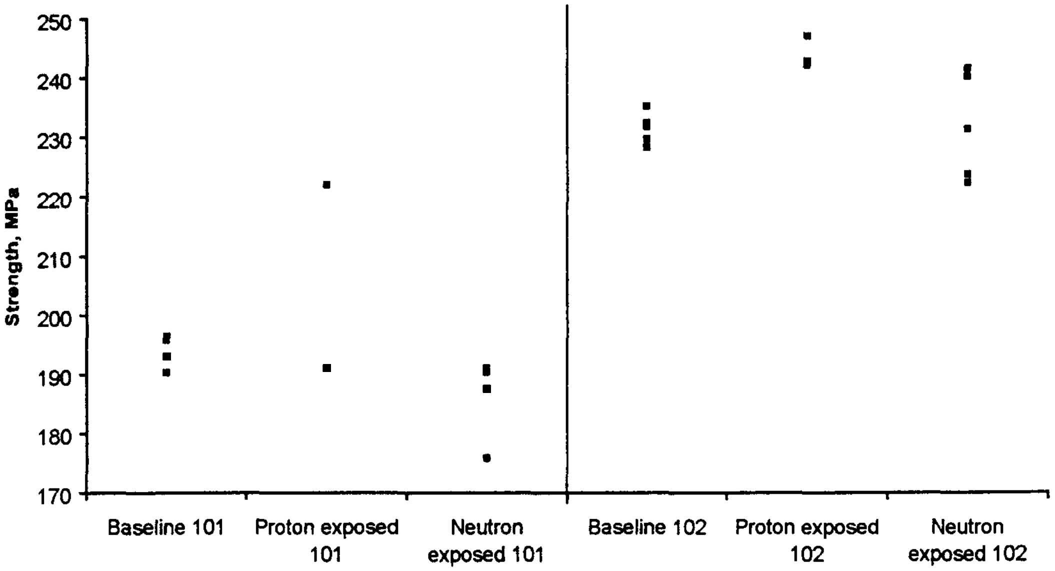

Figure 5(c). Ultimate compressive strength for regolith 101 specimens on left-hand side and for regolith 102 specimens on right-hand side.

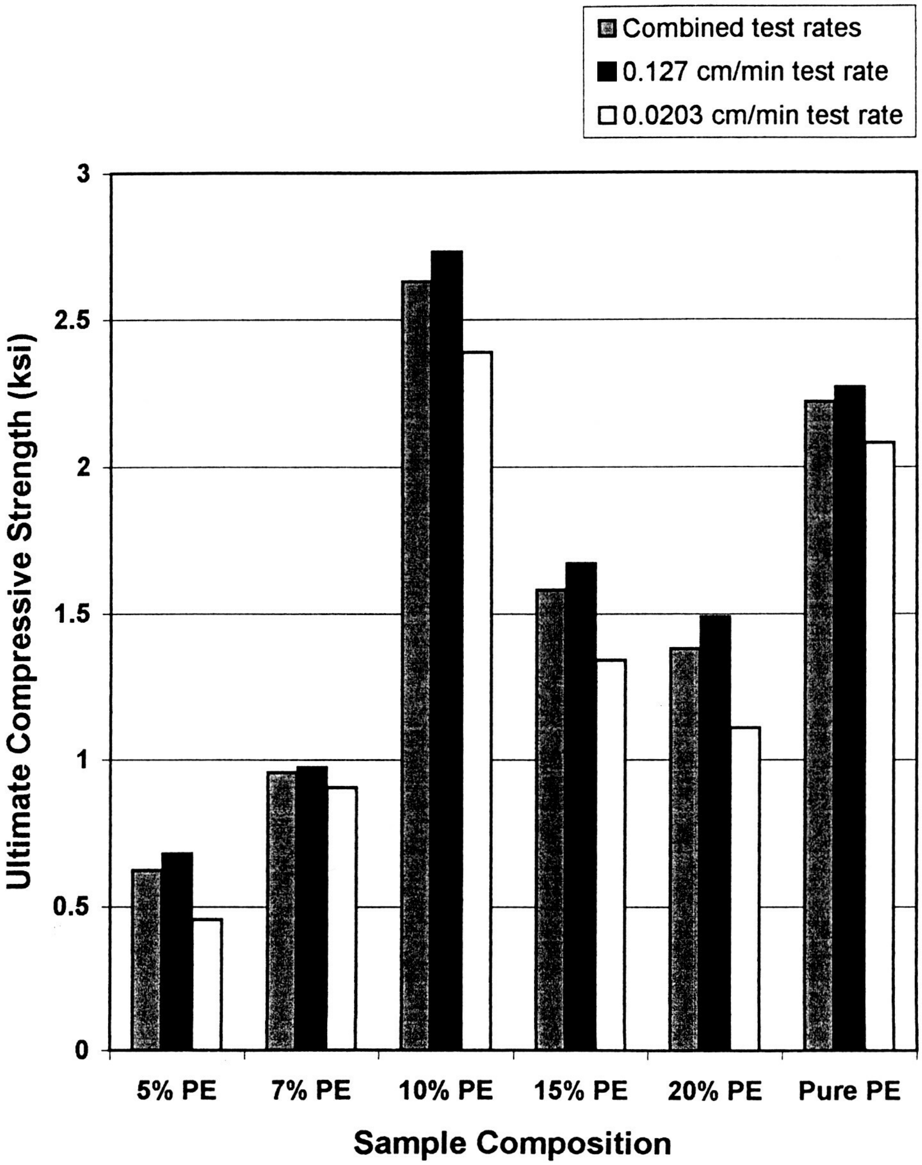

Figure 6. The ultimate compressive strength of polyethylene/regolith composites

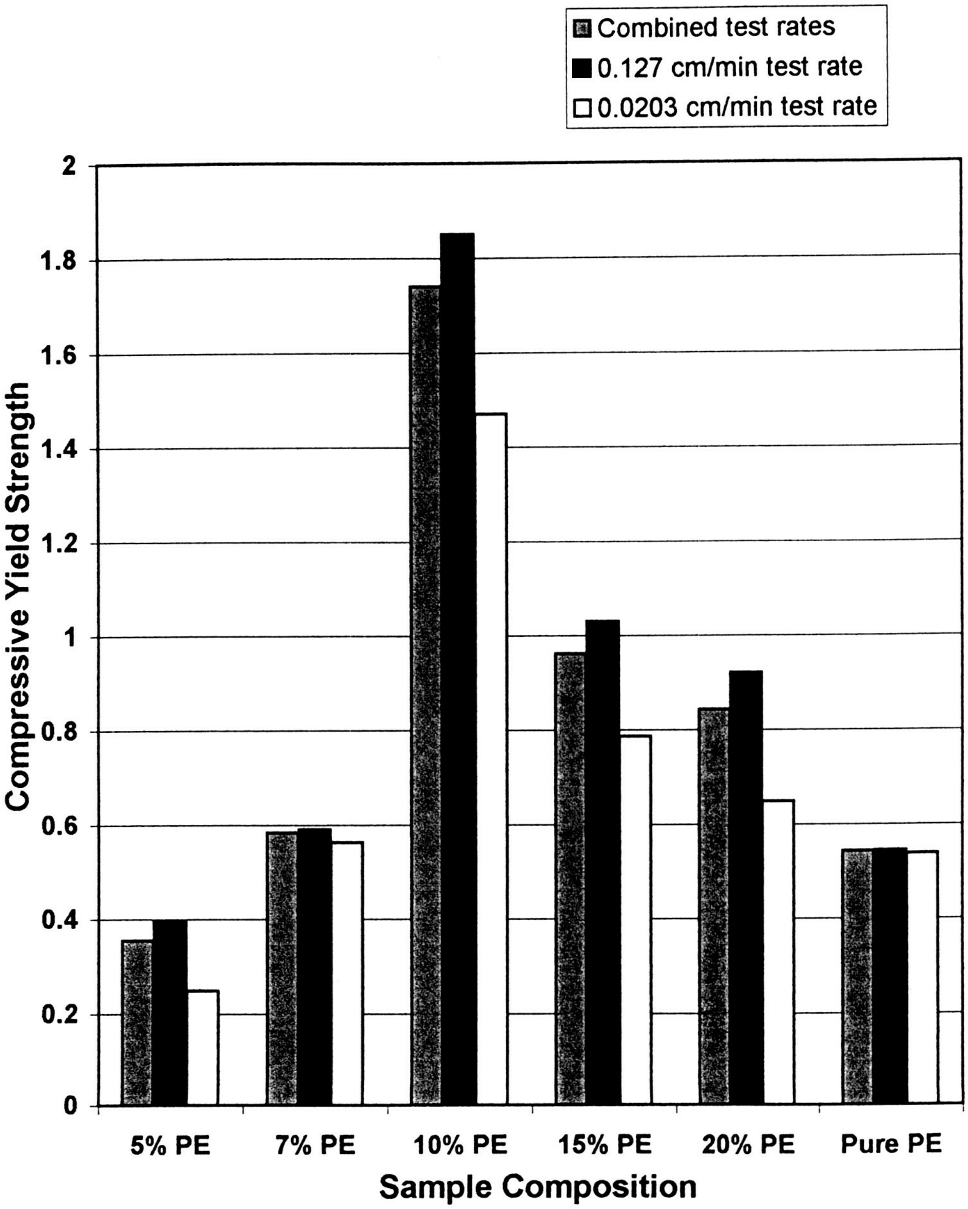

Figure 7. The compressive yield strength for polyethylene/regolith composites

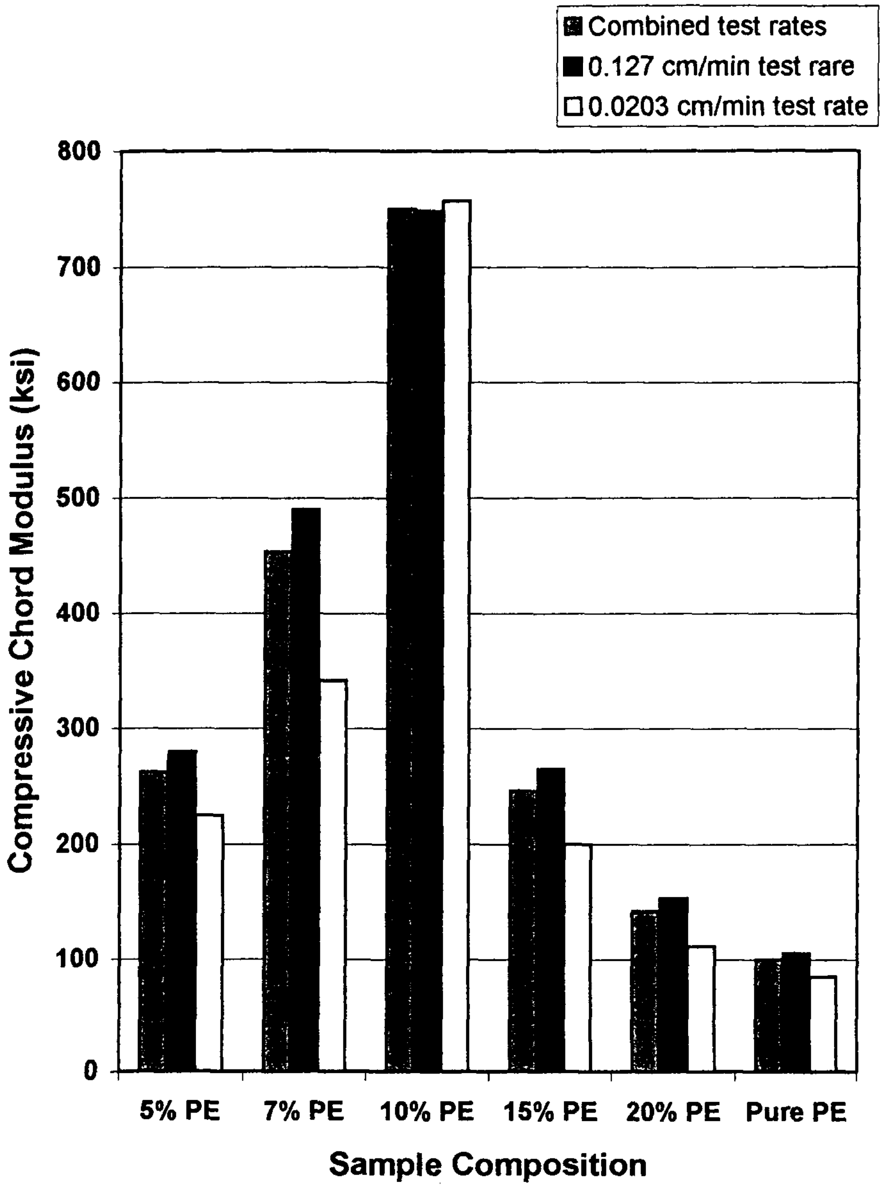

Figure 8. The compressive chord modulus of elasticity for polyethylene/regolith composites

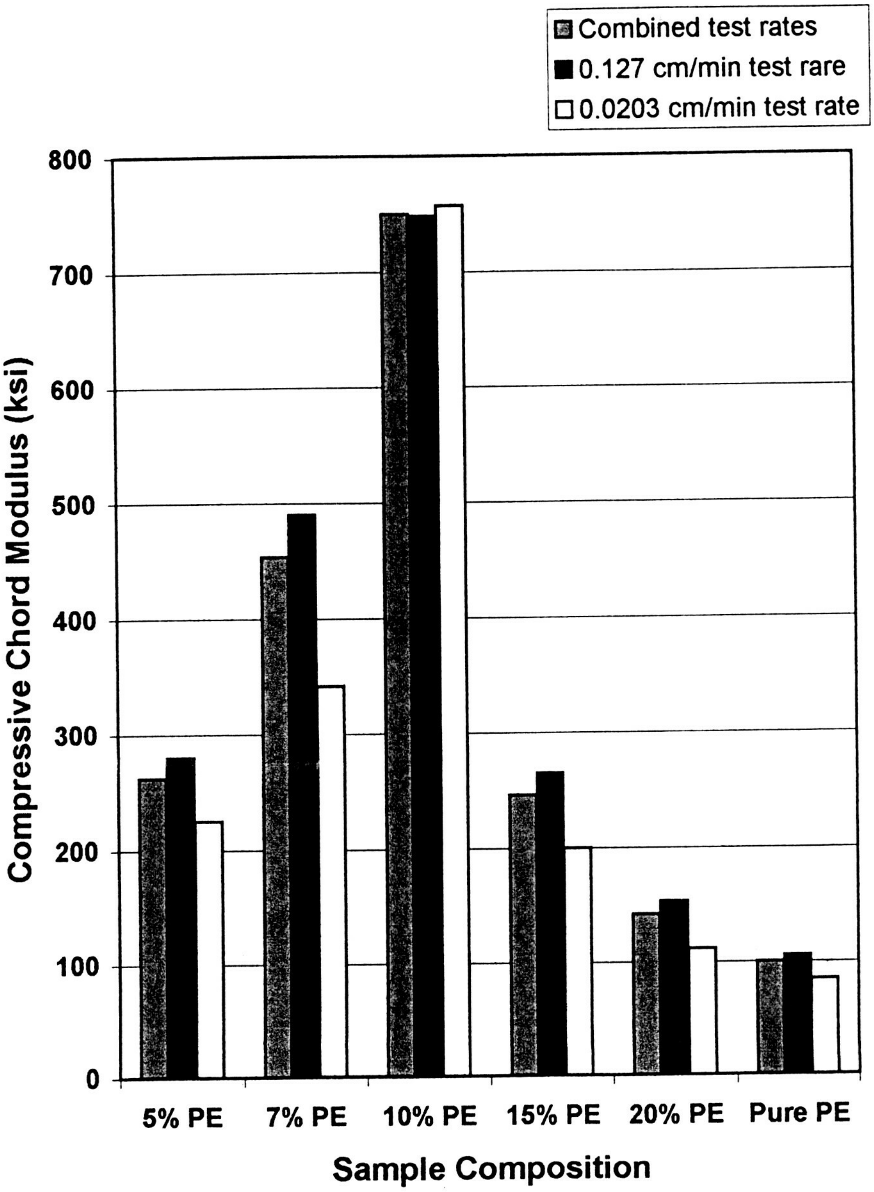

Figure 8. The compressive chord modulus of elasticity for polyethylene/regolith composites